


CLINICAL COMMENTARY

ILAE neuroimaging task force highlight: The utility of multimodal neuroimaging in diagnostic and presurgical workup of drug-resistant focal epilepsy

Niccolò Biagioli^{1,2} | Maksim Parfyonov³ | Stefano Meletti^{1,2} | Giacomo Pavesi⁴ | John Archer⁵ | Boris C. Bernhardt⁶ | Lorenzo Caciagli⁷ | Fernando Cendes⁸ | Yotin Chinvarun⁹ | Luis Concha¹⁰ | Paolo Federico¹¹ | William D. Gaillard¹² | Eliane Kobayashi¹³ | Godwin Ogbole¹⁴ | Stefan Rampp^{15,16} | Shuang Wang¹⁷ | Gavin P. Winston¹⁸ | Irene Wang³  | Anna Elisabetta Vaudano^{1,2}

Correspondence

Irene Wang, Epilepsy Center, Cleveland Clinic, Desk S-51, 9500 Euclid Avenue, Cleveland, OH 44195, USA.
Email: wangi2@ccf.org

Funding information

Sao Paulo Research Foundation (FAPESP) Research Innovation and Dissemination Center, Grant/Award Number: 2013/07559-3; National Institute of Neurological Disorders and Stroke, Grant/Award Number: R01 NS109439

Abstract

The ILAE Neuroimaging Task Force publishes educational case reports that highlight basic aspects of neuroimaging in epilepsy, consistent with ILAE's educational mission. In patients with drug-resistant focal epilepsy who are candidates for surgical intervention, the identification of structural abnormalities is a strong predictor of favorable postoperative seizure outcomes. When conventional imaging is insufficient, the integration of multimodal neuroimaging data with structural, metabolic, and functional imaging modalities is often helpful. The following two illustrative cases from two different centers highlight the challenges and needs to integrate the information from multiple imaging modalities for a more accurate diagnosis and resection planning of drug-resistant focal epilepsies. This approach can increase the number of patients eligible for surgery while minimizing the risk of postoperative deficits.

KEYWORDS

multimodal, MRI-negative, MRI post-processing, nonlesional, presurgical evaluation

1 | CASE 1

1.1 | Clinical history

A 27-year-old right-handed male presented to the Epilepsy Center in Modena, Italy, with drug-resistant

focal epilepsy since the age of 20 years. The patient experienced two distinct seizure types. First, he had brief focal aware seizures characterized by a subjective sensation of a “rhythm in the head,” devoid of emotional connotation or memory evocation followed by a depersonalization described as a sense of estrangement from

Niccolò Biagioli and Maksim Parfyonov are first author equal contribution.

For affiliations refer to page 448.

This is an open access article under the terms of the [Creative Commons Attribution-NonCommercial-NoDerivs](https://creativecommons.org/licenses/by-nc-nd/4.0/) License, which permits use and distribution in any medium, provided the original work is properly cited, the use is non-commercial and no modifications or adaptations are made.

© 2025 The Author(s). *Epileptic Disorders* published by Wiley Periodicals LLC on behalf of International League Against Epilepsy.

the environment and from his own body. These seizures were often spontaneous or triggered by environmental noises. In the latter case, the subjective auditory sensation tended to synchronize with external sounds and bystanders' words. In addition, the patient reported monthly focal seizures occurring during the early stages of sleep (N1-N2 NREM), characterized by abrupt arousal and eye opening, confused gaze, followed by tonic head deviation to the left. This was then accompanied by elevation of the left upper limb, progressing to hyperkinetic bilateral movements. The patient reported becoming retrospectively aware of the event due to the confusion upon awakening that followed the seizure. Despite multiple anti-seizure medications (ASM), the patient continued to have daily focal aware seizures. At the first evaluation, at the age of 23, video-EEG monitoring showed a right frontotemporal focus with occasional slow-wave complex and numerous epileptiform abnormalities with spike or spike-wave morphology. Structural brain MRI at 3T was reported as normal. Given the limited response to ASM and in order to further evaluate the patient's epilepsy for surgical candidacy, the patient was admitted to the Epilepsy Monitoring Unit (EMU) again when he was 27.

1.2 | Comprehensive noninvasive evaluation

1.2.1 | Long-term video-EEG monitoring

Diurnal and nocturnal recordings revealed frequent interictal epileptiform abnormalities, with spikes, polyspikes, and spike-wave isolated or in short runs at the right frontotemporal region (Figure 1A,B). Ictal EEG showed a right frontal onset characterized by a focal flattening of cerebral electrical activity at electrode F8, T4, followed by low-voltage rhythmic fast spike activity at 14–15 Hz over the right anterior frontal and frontotemporal regions, with later spread to the vertex and contralateral fronto-central and frontotemporal areas (Figure 1C). Nocturnal EEG demonstrated electrographic seizures characterized by a slow-wave complex followed by low voltage fast activity and sharp-wave complex in the right frontotemporal regions (Fp2-F8; F8-T4), occasionally leading to patient arousal (Figure 1D). No major seizures with hyperkinetic movements were recorded.

1.2.2 | Noninvasive neuroimaging investigations

MRI (3T, General Electric) included sequences according to the HARNESS protocol¹ including 3D MPRAGE (TR/

Key points

- Identification of subtle structural abnormalities is a strong predictor of favorable postoperative seizure outcomes.
- MRI post-processing techniques effectively enhance the detection of structural abnormalities.
- Integrating multimodal imaging and electrophysiology data within the same three-dimensional space allows for analyzing relationships between these data accurately.
- Multimodal neuroimaging approaches increase diagnostic confidence, especially when abnormalities are subtle or ambiguous.

TE = 2230/3 ms, voxel size 1 × 1 × 1 mm), 3D FLAIR (TR/TE = 6000/117 ms, voxel size 1.2 × 1.2 × 1.2 mm), and coronal T2 perpendicular to the hippocampal axis with high in-plane resolution (TR/TE: 9600/90 ms, 0.4 × 0.4 × 2 mm). In addition, the epilepsy protocol in Modena's Hospital includes a tridimensional pCASL perfusion imaging (Arterial Spin Labelling, ASL; TR/TE = 4854/10.7 ms, slice thickness 4 mm, and Post Label Delay = 2025 ms), an axial 2D diffusion sequence (TR/TE 9140/70, 2 × 1.6 × 3.6 mm), and an axial 2D T2 gradient-echo image (TR/TE 1079.1/13 ms, 0.8 × 1.1 × 3 mm). Visual inspection of MRI images revealed an area of focal hyperintensity and gray-white (GW) matter blurring over the right fronto-opercular region, visible only on the coronal plane and particularly on FLAIR (Figure 2A). This abnormality was initially not reported as a potential lesion on the anatomical MRI. After qualitative visual inspection, the interictal [¹⁸F]Fluorodeoxyglucose Positron Emission Tomography ([¹⁸F]FDG-PET) was reported to show subtle hypometabolism over the right mesial frontal region and right temporal pole. No significant changes were noted in correspondence with the possible lesion observed on MRI (Figure 2B). Visual inspection of the ASL map revealed an extensive area of hypoperfusion over the right frontal region, including the frontal pole and the frontal operculum (Figure 2B).

1.3 | Post-processing analyses and multimodal imaging integration

With a clinical/imaging based hypothesis of a cortical abnormality in the right fronto-opercular region, we undertook post-processing integrative analyses on structural MRI, ASL and metabolic images using an in-house open-source automatic pipeline (namely SWANe

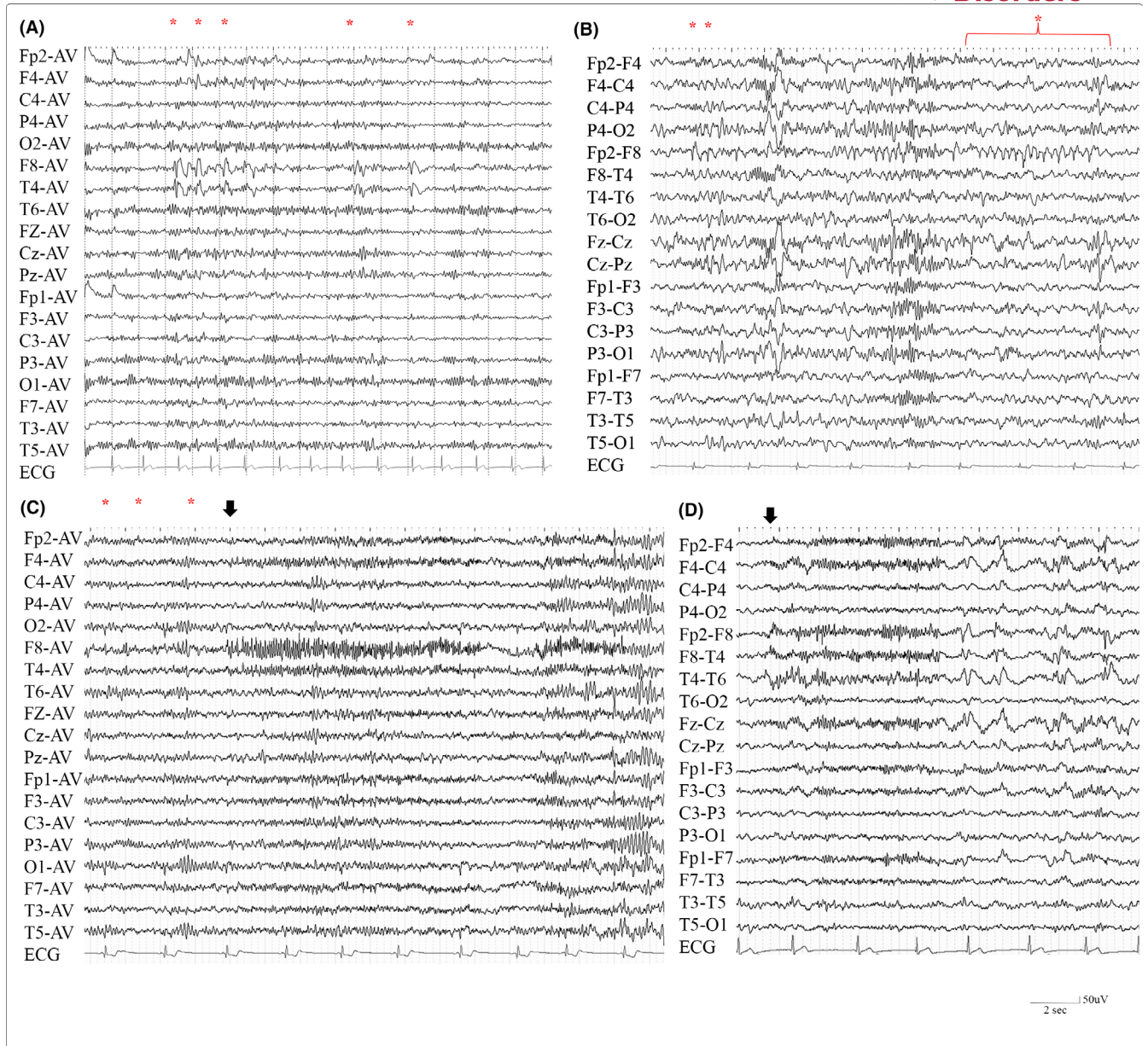
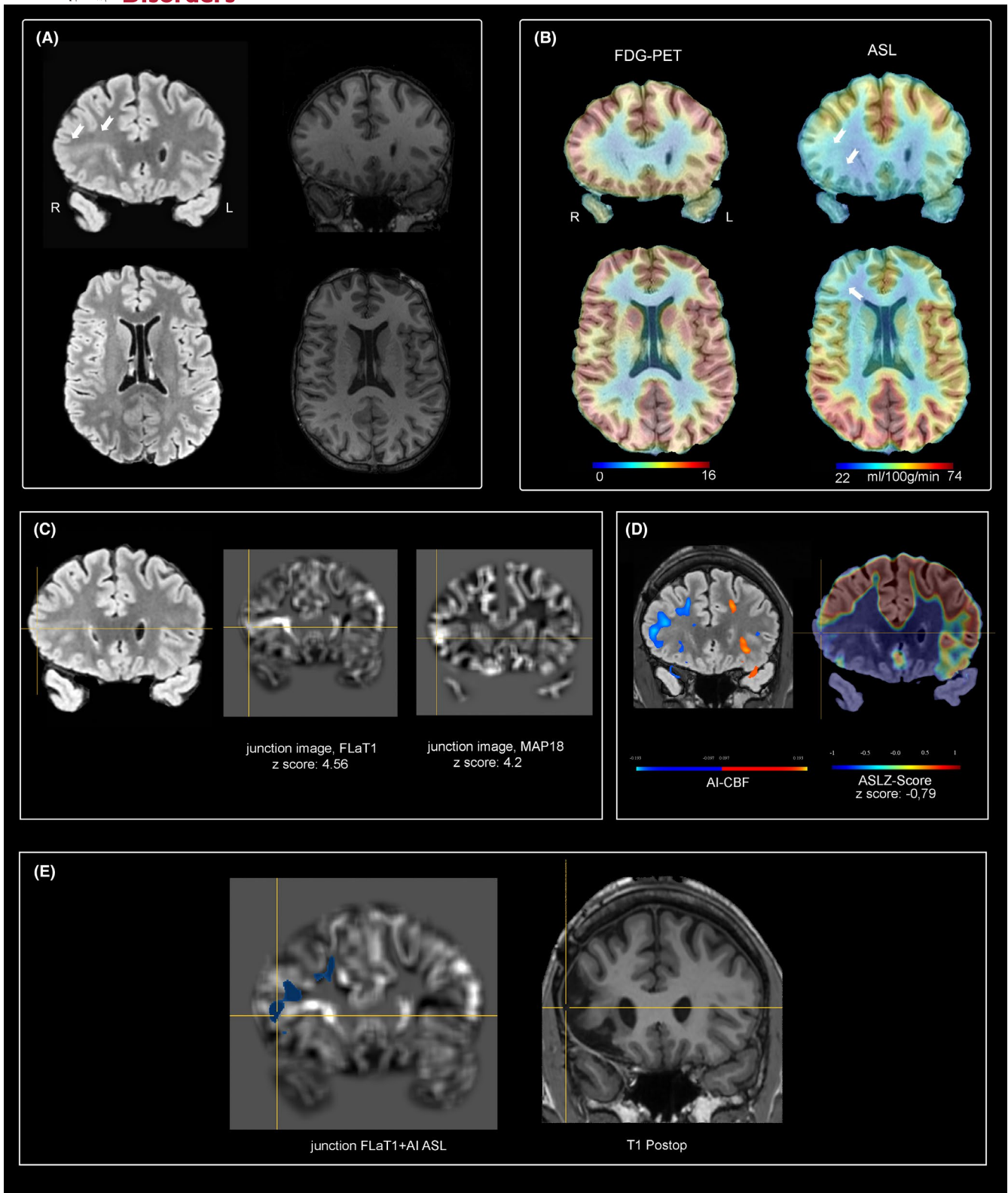


FIGURE 1 Case 1: Neurophysiological findings. (A) Interictal epileptiform discharges. Focal spike-wave and sharp waves in the right frontotemporal region (T4; T6) during wakefulness. Red asterisks highlight EEG abnormalities. EEG trace (30 s page) is shown in a monopolar montage (High-pass filter of 0.1 Hz, Low-pass filter of 35 Hz, Notch filter of 50 Hz). (B) Interictal epileptiform discharges. Focal spike, polyspikes, and sharp waves in the right frontotemporal region (Fp2-F8; F8-T4) while asleep (NREM phase 2). Red asterisks and curly bracket highlight EEG abnormalities. EEG trace (30 s page) is shown in a bipolar montage (High-pass filter of 0.1 Hz, Low-pass filter of 35 Hz, and Notch filter of 50 Hz). (C) Ictal discharges: Right focal aware seizure (black arrow) characterized by low-voltage rapid rhythmic activity at 14–15 Hz over the right frontotemporal region (F8;T4) preceded by isolated spikes over the same territory (red asterisks). EEG trace (30 s page) is shown in average montage (High-pass filter of 0.1 Hz, Low-pass filter of 35 Hz, and Notch filter of 50 Hz). Clinically, the patients reported the habitual subjective sensation of “rhythm in the head.” (D) Nocturnal seizure (Stage N2 NREM): Brief seizures composed by rapid spike-like abnormalities in the right frontal derivations but diffused even in contralateral frontal region, followed by sharp waves and spikes with equipotentiality at F8-T4 electrodes (black arrow). EEG trace (30 s page) is shown in a bipolar montage (High-pass filter of 0.1 Hz, Low-pass filter of 35 Hz, and Notch filter of 50 Hz).

“Standardized Workflow for Advanced Neuroimaging in Epilepsy,”² <https://github.com/LICE-dev/swane/wiki>. T1 and FLAIR 3D images underwent processing using a voxel-based morphometry approach (named FLat1)

that investigates abnormalities of the GW junction and gray-matter (GM) gyration, comparing the patient's 3D-T1 and 3D-FLAIR images with a normative dataset² (see Data S1 for details). FLat1 generates two images:



a junction image and an extension image. When applied to the patient's structural T13D and FLAIR, the junction image obtained from FlaT1 highlighted GW blurring over the right inferior frontal gyrus (Z -score = 4.56) while the extension map was not informative (Z -score = 1.11;

Figure 2C). This area was concordant with the visually detected lesion.

To validate this finding, the native 3D-T1 image was analyzed using the Morphometric Analysis Program (MAP), a widely used voxel-based morphometry tool for

FIGURE 2 Case 1: Multimodal imaging findings and post-processing results. (A) Anatomical FLAIR and T1 high-resolution images from the HARNNESS protocol displayed in coronal and axial orientation. The coronal FLAIR image shows a region of gray-white matter blurring and a transmantle sign at the right frontal cortex (pars triangularis of the inferior frontal gyrus) (white arrows). L = Left; R = Right. (B) FDG-PET (left images) and ASL-CBF maps (right images) overlaid onto the anatomical T1 image (coronal and axial slices). While the FDG-PET is not clearly informative at qualitative visual inspection for significant hypometabolic areas, the ASL-CBF map inspected visually shows a clear diffuse hypoperfusion over the right frontal pole and fronto-dorsolateral cortex (white arrows). (C) Post-processing analyses on anatomical MRI sequences using FLAT1 and MAP18. From left to right: Representative presurgical coronal FLAIR slice, with the yellow cross highlighting the presumed lesion; junction map obtained from FLAT1 program coregistered with the anatomical FLAIR sequence; junction map obtained from MAP18 program coregistered with the anatomical FLAIR sequence. (D) Post-processing analyses on the ASL images. From left to right: AI-ASL CBF maps overlaid onto the presurgical coronal FLAIR image; Z-score ASL maps overlaid onto the presurgical coronal FLAIR image. The yellow cross indicates the area of FLAT1 positive finding. (E) Multimodal imaging integration. From left to right: ASL asymmetry index map overlaid onto the junction map obtained from FLAT1 program; postsurgical coronal T1 image. The yellow cross highlights the lesion area of FLAT1 positive finding.

the investigation of focal cortical dysplasia (FCD).^{3,4} MAP showed concordant areas of signal abnormality in the junction map (Z-score = 4.2), while the extension map was not informative (Figure 2C).

The ASL-CBF and FDG-PET images underwent two quantitative approaches, both exploring differences in perfusion and metabolism at the voxel level without the need for normative data. These analyses estimate respectively the asymmetry index (AI) and the mean and standard deviation of ASL and PET values with respect to the basal ganglia, generating z-score maps (see Data S1). The AI and z-score analyses on ASL emphasize the hypoperfusion over the right frontal operculum (Figure 2D) while the AI and Z-score analysis of PET images was not informative (Figure S1).

Using the SWANe pipeline, all relevant neuroradiological data from the above investigations (structural MRI sequences, FDG-PET and ASL images, results of post-processing analyses) were co-registered to the anatomical T1w image and integrated into a multimodal platform. The resulting multimodal scene (Figure 2E) informed the multidisciplinary patient management conference (PMC) discussion, leading to a consensus to proceed with the resection of the suspected abnormality guided by intraoperative electrocorticography. Neuropathological examination of the resected tissue revealed diffuse gliosis without distinct cellular dysmorphisms or atypia. At 24-month post-surgical follow-up, the patient remained seizure-free and ASM was gradually being reduced.

2 | CASE 2

2.1 | Clinical history

An 18-year-old right-handed male with a history of drug-resistant focal epilepsy was referred for presurgical evaluation at the Cleveland Clinic Epilepsy Center, USA. His

parents initially noticed episodes of staring and infrequent right eye fluttering in early childhood. Definite seizures began at age 8, with nocturnal tonic seizures characterized by “body stiffening” with bilateral flexion of arms and legs, followed by rocking movements and drooling. Seizures continued monthly despite multiple trials of appropriately dosed ASMs.

2.2 | Comprehensive noninvasive evaluation

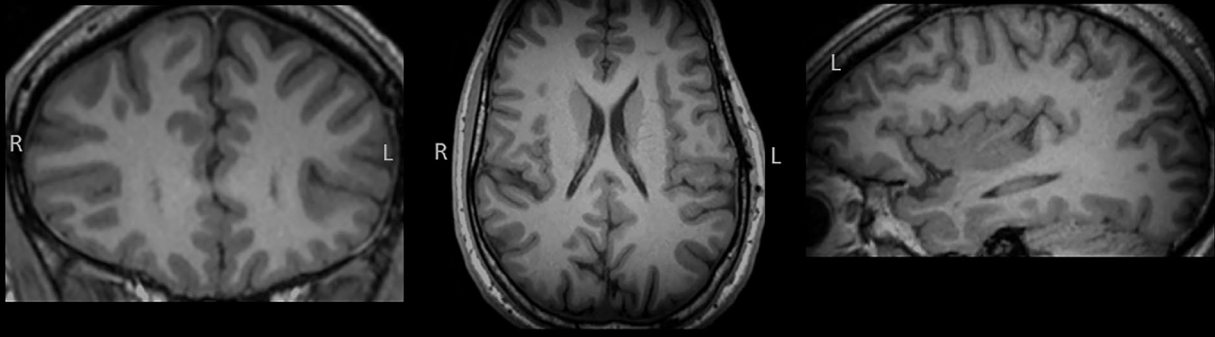
2.2.1 | Long-term video-EEG monitoring

Interictal EEG showed intermittent generalized slowing and frequent left frontotemporal sharp waves (maximum F7, T7, and FT7), often occurring in runs. Several seizures were recorded, with onset marked by left frontotemporal fast activity or sharp wave, followed by quick propagation of theta activity to the vertex and spread to both hemispheres. Clinically, all seizures occurred during sleep and were characterized by arousal, forward movement of the head and shoulders with bilateral leg extension, and vocalization in the form of a high-pitched, repetitive sound, as if whining. Rarely, some seizures progressed to bilateral tonic-clonic movements.

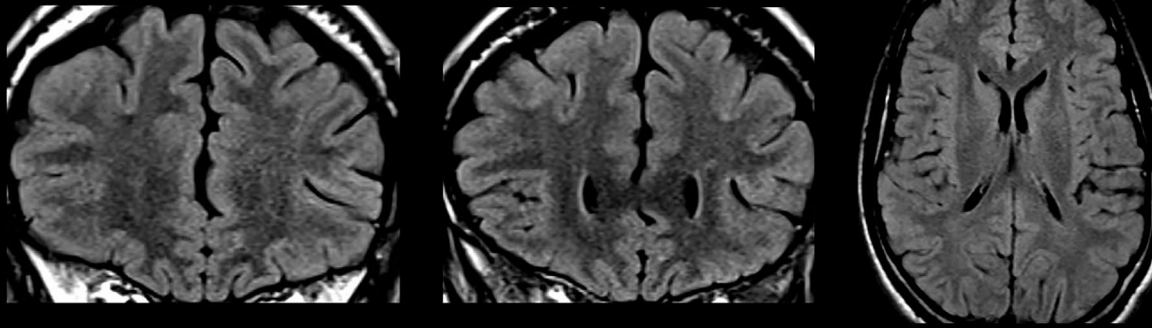
2.2.2 | Noninvasive neuroimaging investigations

An epilepsy-protocol MRI was performed using a 3T Siemens scanner, including sequences aligned with the HARNNESS protocol, and was interpreted as negative by the official radiology report (Figure 3A,B). FDG-PET showed left greater than right temporal and left lateral frontal hypometabolism (Figure 3C). Source analysis of interictal magnetoencephalography (MEG) data revealed

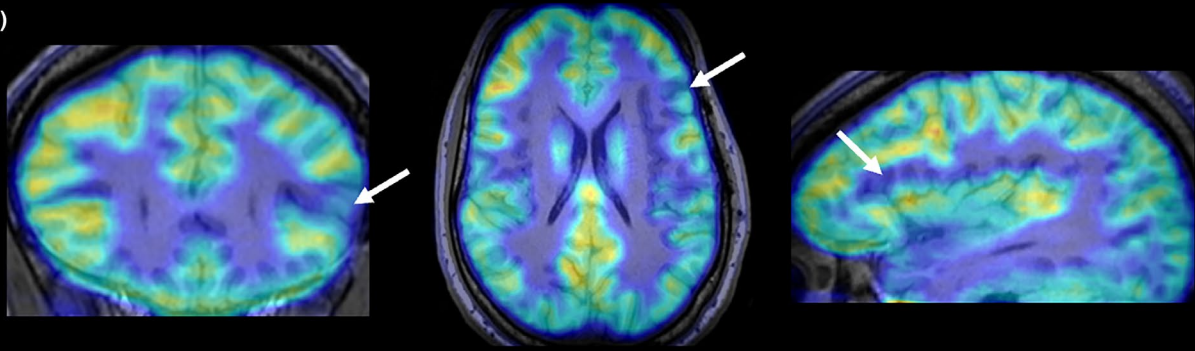
(A)



(B)



(C)



(D)

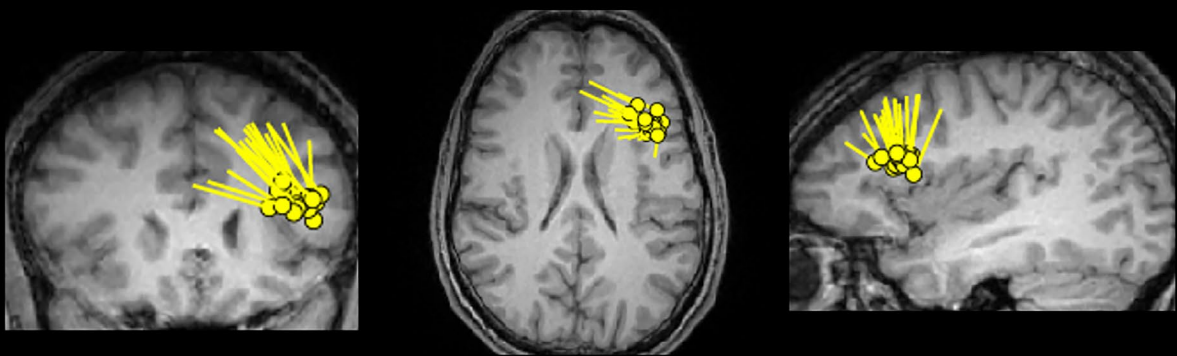


FIGURE 3 Case 2: Presurgical multimodal data from the initial evaluation. (A) 3T T1w MRI in coronal, axial, and sagittal planes, initially reported as nonlesional. (B) 3T FLAIR in two coronal slices and one coronal slice near the subtle abnormality later identified. In retrospect, some features of FCD are discernible on these slices; however, they were too subtle to identify prospectively without post-processing assistance. (C) FDG-PET showing hypometabolism in the left inferior frontal gyrus. Arrows point to the hypometabolic regions pertinent to the subtle abnormality later identified. (D) Source localization of interictal dipoles on magnetoencephalography (MEG).

a tight cluster of dipoles in the left inferior frontal region (Figure 3D). Ictal SPECT was attempted, but late injection precluded accurate interpretation. Functional MRI showed predominantly left-sided speech activation.

2.3 | Intracranial evaluation

The patient underwent a subdural grid and depth electrode evaluation (Figure 4A). Interictal epileptiform abnormalities were recorded from the left inferior frontal gyrus and left mesiobasal and anterior temporal regions. The ictal pattern was seen earliest over the left inferior frontal gyrus on grid electrodes SB14, 15, 19, and 20 (red electrode contacts, Figure 4A), characterized by repetitive spiking (Figure 4G). This evolved to low amplitude fast activity in these regions, followed by rhythmic theta-alpha activity spreading to neighboring electrodes in the frontal and temporal regions (Figure 4H). Language areas shown by cortical stimulation were mapped to SB14, 15, 19, 24, 25, and SA32, 36 (red and purple electrode contacts, Figure 4A), with partial overlap of the seizure onset zone electrodes.

The above presurgical noninvasive and invasive data were reviewed at the interdisciplinary PMC. Due to the proximity of the ictal onset zone to the eloquent cortex, concerns were raised for incurring a language deficit with resection. Surgery was therefore deferred by the patient.

2.4 | Post-processing analyses and multimodal imaging integration

The patient returned to Cleveland Clinic Epilepsy Center for reevaluation 10 years later due to increased seizure burden. By this time, MRI post-processing techniques and multimodal imaging techniques were established and integrated into clinical use, particularly for nonlesional MRI cases. MRI post-processing was performed using MAP^{3,4} on 3T MRI, which revealed subtle blurring of the GW junction (Z -score = 4.1) at the bottom of an accessory sulcus in the left pars triangularis, suggestive of a bottom-of-sulcus FCD (Figure 4B–D). This abnormality was visible upon rereview of the original clinical MRI by a neuroradiologist during PMC. 7T MRI also recapitulated the lesion on T1w and T2*w sequences (Figure 4E,F). Identification

of this lesion prompted a re-review of the data from the previous evaluation using multimodal image integration. MRI, MAP, PET, MEG, and invasive EEG (locations of ictal onset and findings from cortical stimulation) were integrated in three-dimensional space using the Curry platform (Compumedics Neuroscan™, Charlotte, NC, USA).⁵ Careful review of the invasive electrode positions revealed that ictal onset electrodes SB14, 15, 19, and 20 were located at the convexity of the subtle bottom-of-sulcus lesion (Figure 4B), likely capturing an exit pattern of epileptic activities. There were no electrodes exactly sampling the subtle abnormality. The closest depth electrode to the lesion was LMF (located 8 mm away from the abnormality). The lateral contacts of LMF showed low-voltage fast activities after the onset (Figure 4G, dashed arrow), which evolved later into the seizure (Figure 4H). The abnormality was separated from the language areas defined by the electrodes causing speech disturbance during stimulation (estimated distance 18.5 mm; Figure 4B). Based on these data, a consensus was reached to proceed with the resection of the lesion with intraoperative monitoring, without another invasive evaluation. The patient underwent an awake craniotomy and electrocorticography-guided resection of the lesion, histopathologically confirmed as FCD IIb. The patient remained seizure-free without a language deficit for more than 5 years postoperatively.

3 | DISCUSSION

The present cases highlight the role of MRI post-processing and multimodal image integration in surgical evaluations, particularly in patients initially classified as MRI-negative by conventional MRI visual inspection. Lesion detection remains a significant challenge in such patients, as some malformations present with very subtle MRI features, which can be missed without the use of optimized sequences and post-processing techniques or if not interpreted by a dedicated neuroradiologist with expertise in epilepsy. The identification of an epileptogenic lesion is one of the main factors influencing the prognosis for epilepsy surgery.⁶ The HARNESS¹ protocol has been demonstrated to identify a higher number of potentially epileptogenic lesions, particularly FCD.⁷ Based on a good-quality MRI compliant with the HARNESS protocol, MRI post-processing analyses are often helpful to direct

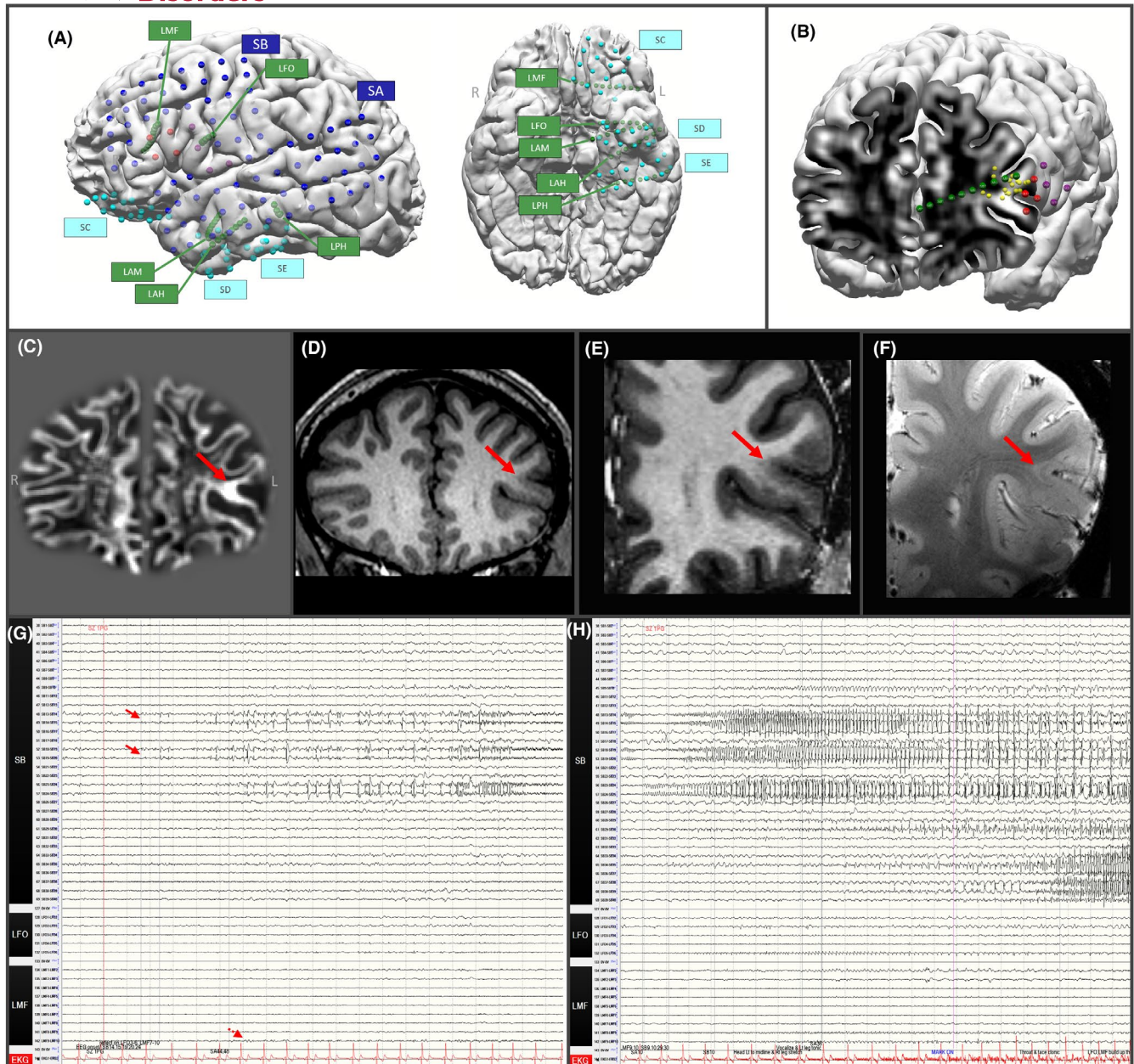


FIGURE 4 Case 2: Intracranial EEG data from the initial evaluation and data for reevaluation. (A) 3D-reconstruction of subdural grids (blue), strips (light blue), and depth electrodes (green) placement in the left hemisphere. (B) Multimodal integration of 3D cortical surface, MAP junction file showing the bottom-of-sulcus lesion, with pertinent electrodes from the previous invasive evaluation. Cut plane corresponds to the subtle lesion detected by MAP. For A and B, colors of spheres are as follows: Red = contacts at seizure onset; Yellow = MEG dipoles; Purple = contacts with speech disturbances during cortical stimulation. (C) Coronal view of MAP gray-white junction file based on 3T T1w MRI (shown in D), highlighting the subtle abnormality in the left inferior frontal region. (D) Coronal 3T T1w image at the same slice of (C). (E) Zoomed in view of the subtle abnormality on coronal 7T T1w MP2RAGE image. (F) Zoom in view of the subtle abnormality on coronal 7T T2* GRE image. (G, H) Intracranial EEG tracing at the onset (G), and 15s of seizure (H) arising from the left inferior frontal region (SB 14–15, 19–20, red arrows). The closest depth electrode to the subtle abnormality was LMF, and low-voltage fast activities were seen on the lateral contacts of LMF (dashed arrow), later than the onset.

clinical attention to previously overlooked brain regions, thereby uncovering structural abnormalities aligned with electroclinical findings. In Case 1, while the FLAIR sequence highlighted a signal alteration in the right fronto-opercular region (Figure 2A), it was not initially

considered significant by expert neuroradiologists. This was primarily because the signal alteration was distinctly observable only in the coronal plane, not on axial or sagittal views. Additionally, the T1w anatomical images provided limited diagnostic value. However, after employing

multimodal imaging modalities and post-processing techniques, the lesional area was later highlighted, prompting a reassessment of the structural MRI findings. In Case 2, reevaluation with MRI post-processing and integration with invasive data 10 years after the initial evaluation highlights the evolving nature of neuroimaging technology. The detection of the subtle bottom-of-sulcus FCD was directly facilitated by MAP and later confirmed on 7T MRI, techniques that were unavailable during the patient's initial evaluation.

MRI post-processing methods have been reported to effectively identify subtle lesions in previously MRI-negative patients. MAP is a widely used method that uses voxel-based morphometric analysis on 3D T1w images and generates three volumetric statistical maps that highlight areas of abnormal gray-white blurring, extension, and cortical thickness.⁴ In Case 1, FlaT1, a custom-built method still in the validation phase² was used alongside MAP. While the input is different, FlaT1 and MAP provided concordant findings. In addition to retrospective studies,^{3,8,9} the value of MRI post-processing techniques for presurgical evaluation has been confirmed by prospective studies.¹⁰ MRI post-processing methods should be incorporated into routine practice at tertiary epilepsy centers, where nonlesional MRI cases are common. Recently, open access tools like MELD¹¹ and DeepFCD¹² implemented machine-learning algorithms for automated detection of FCD, further assisting clinicians in the identification of subtle MRI lesions in individuals with epilepsy. Of note, since these approaches are not CE/FDA approved, results must be interpreted with caution by qualified staff with expertise in computational anatomy and imaging processing and corroborated by clinical information and other imaging data. The broader adoption of these approaches in resource-constrained settings also faces challenges due to several factors, including licensing restrictions, computational requirements, and the need for specialized training.

ASL is a useful functional neuroimaging modality, well recognized to be helpful in the localization of the EZ.¹³⁻¹⁵ Unlike FDG-PET, it is a noninvasive method that uses magnetic-labeled blood as an endogenous tracer to generate quantitative maps of cerebral blood flow, particularly useful for studying children.^{14,16} In Case 1, ASL revealed significant hypoperfusion in the right inferior fronto-opercular/frontal region, spatially concordant with the potential structural lesion. For quantitative analysis, ASL data were expressed as an estimation of the asymmetry index, which highlights variations in perfusion at each voxel, comparing one hemisphere with its contralateral counterpart in the same patient. This approach is particularly useful for identifying hyper/hypoperfused brain areas in the presurgical evaluation of children with focal epilepsy.^{14,17}

The visual review of FDG-PET was concordant with the subtle structural lesion in Case 2, while for Case 1, even when coregistered with the structural MRI and after using post-processing, PET was uninformative. This may reflect the reduced localizing value of PET in extratemporal lobe epilepsies.¹⁸ Additionally, PET findings may appear pseudo-normal if increased epileptic activity leads to hypermetabolism in an otherwise hypometabolic area. In Case 1, the PET scan was acquired at a different time than the structural MRI protocol (including ASL). Notably, the scalp EEG performed just before the PET scan showed significant activity, despite no seizures being recorded. This observation highlights the importance of recording scalp EEG before or during radiotracer uptake to aid PET interpretation.¹⁹

Equally important in both patients was the integration of multiple imaging data into a common 3D space, enabling simultaneous visualization of all modalities, evaluating their interrelationships and level of concordance.^{5,20} Concordant results from one modality may prompt a focused reevaluation of another; this iterative review process allows modalities to inform one another, improving diagnostic yield. For Case 2, overlaying cortical stimulation data on the 3D space helped reveal the spatial relationship between eloquent brain regions and the ictal onset zone. Reevaluating data using this method in this case demonstrated that the tight cluster of MEG dipoles overlapped with the subtle lesion, adding an electrophysiological correlate to the structural abnormality. The bottom of the sulcus lesion location could explain the exit pattern of ictal onset on the subdural grids (as well as the later-appearing low voltage fast activities in the nearest depth electrode [Figure 4G, dashed arrow]). Visualizing cortical stimulation findings in 2D and 3D clarified the relationship between ictal onset, the structural lesion, and language areas. This knowledge enabled successful lesionectomy while sparing language function. By multimodal integration, invasive EEG data were maximally utilized, so that the patient did not have to undergo another intracranial EEG evaluation, thereby reducing costs and mitigating the risks of complications.

Multimodal integration is crucial for forming and refining the electroclinical hypothesis and surgical strategy, particularly relevant for SEEG. Given the "tunnel vision" nature of SEEG, its success heavily depends on the preimplantation accuracy, often facilitated by multimodal integration. Multimodal integration has led to significant changes in invasive EEG planning and surgical strategies, including electrode placement and trajectory planning. In a prospective study of 44 patients, multimodal integration data changed the surgical strategy in about one third of cases and altered trajectory planning in 80% of cases, primarily in SEEG patients.²⁰ Moreover, multimodal integration can

be valuable for evaluating complex cases with previous surgical failures or patients previously deemed unsuitable for surgery. A prior study demonstrated that careful review of presurgical MRI, enhanced by post-processing methods, identified lesions in 27% of 56 MR-negative patients who had failed initial surgery.²¹ Integration of additional modalities, such as MEG and SPECT, can provide additional detail in interpreting epileptogenicity in surgical failure cases.²² Additionally, integrating postoperative scans from the prior surgery allows for the visualization of the resection cavity's relationship to presurgical data, facilitating a comprehensive evaluation.⁵

4 | CONCLUSION

The two cases presented here highlight the role of advanced imaging techniques and multimodal integration in evaluating MRI-negative focal epilepsy. MRI post-processing techniques significantly enhance the detection of subtle abnormalities, while multimodal integration can increase diagnostic confidence, especially when abnormalities are subtle or ambiguous. Continued research and refinement of multimodal approaches hold promise for advancing our understanding and management of drug-resistant focal epilepsies. Future efforts should focus on optimizing these tools for wider accessibility, including the development of user-friendly, open-source workflows, and targeted training programs for clinicians in diverse practice settings.

AFFILIATIONS

¹Neurophysiology Unit and Epilepsy Centre, University of Modena and Reggio Emilia, Modena, Italy

²Department of Biomedical, Metabolic, and Neural Sciences, Center for Neuroscience and Neurotechnology, University of Modena and Reggio Emilia, Modena, Italy

³Epilepsy Center, Neurological Institute, Cleveland Clinic, Cleveland, Ohio, USA

⁴Neurosurgery Unit, University of Modena and Reggio Emilia, Modena, Italy

⁵Department Medicine, Austin Health, The University of Melbourne, Melbourne, Australia

⁶Multimodal Imaging and Connectome Analysis Laboratory, McConnell Brain Imaging Centre, Montreal, Canada

⁷Department of Neurology, Inselspital, Sleep-Wake-Epilepsy-Center, Bern University Hospital, University of Bern, Bern, Switzerland

⁸Department of Neurology, University of Campinas - UNICAMP, Campinas, SP, Brazil

⁹Epilepsy Center, Neurology Unit, Phramongkutklao Hospital, Bangkok, Thailand

¹⁰Institute of Neurobiology, Universidad Nacional Autónoma de México, Mexico City, Mexico

¹¹Hotchkiss Brain Institute, Cumming School of Medicine, University of Calgary, Calgary, Canada

¹²Center for Neuroscience, Children's National Hospital, George

Washington University, Washington, DC, USA

¹³Department of Neurology, Southwestern Peter O'Donnell Jr. Brain Institute, University of Texas, Dallas, Texas, USA

¹⁴Department of Radiology, University of Ibadan, Ibadan, Nigeria

¹⁵Department of Neurosurgery and Department of Neuroradiology, University Hospital Erlangen, Erlangen, Germany

¹⁶Department of Neurosurgery, University Hospital Halle (Saale), Halle, Germany

¹⁷Department of Neurology and Epilepsy Center, Zhejiang University, Hangzhou, China

¹⁸Division of Neurology, Department of Medicine, Queen's University, Kingston, Canada

ACKNOWLEDGMENTS

FC is supported by Sao Paulo Research Foundation (FAPESP) Research Innovation and Dissemination Center grant 2013/07559-3. ZIW is supported by the National Institutes of Health (R01 NS109439).

DATA AVAILABILITY STATEMENT

The data that support the findings of this study are available on request from the corresponding author. The data are not publicly available due to privacy or ethical restrictions.

ORCID

Irene Wang  <https://orcid.org/0000-0002-3829-5217>

REFERENCES

1. Bernasconi A, Cendes F, Theodore WH, Gill RS, Koepp MJ, Hogan RE, et al. Recommendations for the use of structural magnetic resonance imaging in the care of patients with epilepsy: a consensus report from the international league against epilepsy neuroimaging task force. *Epilepsia*. 2019;60(6):1054–68. <https://doi.org/10.1111/epi.15612>
2. Genovese M, Arcasensa A, Morbelli S, Lenge M, Barba C, Mirandola L, et al. SWANe: standardized workflow for advanced neuroimaging in epilepsy. *SoftwareX*. 2024;26:101703. <https://doi.org/10.1016/j.softx.2024.101703>
3. Wagner J, Weber B, Urbach H, Elger CE, Rgen Huppertz H-J, Huppertz H-J. Morphometric MRI analysis improves detection of focal cortical dysplasia type II. *Brain*. 2011;134(10):2844–54.
4. Huppertz HJ, Wellmer J, Staack AM, Altenmüller DM, Urbach H, Kröll J, et al. Voxel-based 3D MRI analysis helps to detect subtle forms of subcortical band heterotopia. *Epilepsia*. 2008;49(5):772–85.
5. Jin L, Choi JY, Bulacio J, Alexopoulos AV, Burgess RC, Murakami H, et al. Multimodal image integration for epilepsy presurgical evaluation: a clinical workflow. *Front Neurol*. 2021;12:709400.
6. Tellez-Zenteno JF, Hernandez Ronquillo L, Moien-Afshari F, Wiebe S. Surgical outcomes in lesional and non-lesional epilepsy: a systematic review and meta-analysis. *Epilepsy Res*. 2010;89(2–3):310–8.
7. Vaudano AE, Ballerini A, Zucchini F, Micalizzi E, Scolastico S, Talami F, et al. Impact of an optimized epilepsy surgery imaging protocol for focal epilepsy: a monocentric prospective study. *Epileptic Disord*. 2023;25(1):45–56.

8. Wang ZI, Jones SE, Jaisani Z, Najm IM, Prayson RA, Burgess RC, et al. Voxel-based morphometric magnetic resonance imaging (MRI) postprocessing in MRI-negative epilepsies. *Ann Neurol*. 2015;77(6):1060–75.
9. Wong-Kisiel LC, Tovar Quiroga DF, Kenney-Jung DL, Witte RJ, Santana-Almansa A, Worrell GA, et al. Morphometric analysis on T1-weighted MRI complements visual MRI review in focal cortical dysplasia. *Epilepsy Res*. 2018;140:184–91.
10. El Tahry R, Santos SF, Vrielynck P, De Tourtchaninoff M, Duprez T, Vaz GR, et al. Additional clinical value of voxel-based morphometric MRI post-processing for MRI-negative epilepsies: a prospective study. *Epileptic Disord*. 2020;22(2):1–9.
11. Spitzer H, Ripart M, Whitaker K, D'Arco F, Mankad K, Chen AA, et al. Interpretable surface-based detection of focal cortical dysplasias: a multi-centre epilepsy lesion detection study. *Brain*. 2022;145(11):3859–71.
12. Gill RS, Lee HM, Caldaïrou B, Hong SJ, Barba C, Deleo F, et al. Multicenter validation of a deep learning detection algorithm for focal cortical dysplasia. *Neurology*. 2021;97(16):E1571–E1582. <https://doi.org/10.1212/WNL.0000000000012698>
13. Kojan M, Gajdoš M, Říha P, Doležalová I, Řehák Z, Rektor I. Arterial spin labeling is a useful MRI method for presurgical evaluation in MRI-negative focal epilepsy. *Brain Topogr*. 2021;34(4):504–10.
14. Tortora D, Cataldi M, Severino M, Consales A, Pacetti M, Parodi C, et al. Comparison of qualitative and quantitative analyses of MR-arterial spin labeling perfusion data for the assessment of pediatric patients with focal epilepsies. *Diagnostics*. 2022;12(4):1–15.
15. Ngo A, Royer J, Rodriguez-Cruces R, Xie K, Dekraker J, Auer H, et al. Associations of cerebral blood flow patterns with gray and white matter structure in patients with temporal lobe epilepsy. *Neurology*. 2024;103(3):1–13.
16. Pasca L, Sanvito F, Ballante E, Totaro M, Paoletti M, Bergui A, et al. Arterial spin labelling qualitative assessment in paediatric patients with MRI-negative epilepsy. *Clin Radiol*. 2021;76(12):942.e15–942.e23.
17. Boscolo Galazzo I, Mattoli MV, Pizzini FB, De Vita E, Barnes A, Duncan JS, et al. Cerebral metabolism and perfusion in MR-negative individuals with refractory focal epilepsy assessed by simultaneous acquisition of 18F-FDG PET and arterial spin labeling. *NeuroImage Clin*. 2016;11:648–57.
18. Burneo JG, Poon R, Kellett S, Snead OC. The utility of positron emission tomography in epilepsy. *Can J Neurol Sci*. 2015;42(6):360–71.
19. Juhász C, John F. Utility of MRI, PET, and ictal SPECT in presurgical evaluation of non-lesional pediatric epilepsy. *Seizure*. 2020;77:15–28.
20. Nowell M, Rodionov R, Zombori G, Sparks R, Winston G, Kinghorn J, et al. Utility of 3D multimodality imaging in the implantation of intracranial electrodes in epilepsy. *Epilepsia*. 2015;56(3):403–13. <https://doi.org/10.1111/epi.12924>
21. Wang ZI, Suwanpakdee P, Jones SE, Jaisani Z, Moosa AN, Najm IM, et al. Re-review of MRI with post-processing in nonlesional patients in whom epilepsy surgery has failed. *J Neurol*. 2016;263(9):1736–45.
22. El Tahry R, Wang ZI, Thandar A, Podkorytova I, Krishnan B, Tousseyn S, et al. Magnetoencephalography and ictal SPECT in patients with failed epilepsy surgery. *Clin Neurophysiol*. 2018;129(8):1651–7.

SUPPORTING INFORMATION

Additional supporting information can be found online in the Supporting Information section at the end of this article.

How to cite this article: Biagioli N, Parfyonov M, Meletti S, Pavesi G, Archer J, Bernhardt BC, et al. ILAE neuroimaging task force highlight: The utility of multimodal neuroimaging in diagnostic and presurgical workup of drug-resistant focal epilepsy. *Epileptic Disord*. 2025;27:439–450. <https://doi.org/10.1002/epd2.70016>

Test yourself

1. How does the morphometric analysis program (like MAP) help in presurgical evaluation?
 - A. Converts EEG morphology into images to aid in localizing surgical onset
 - B. Improves detection of blurred gray-white matter junctions associated with FCD
 - C. Creates size estimates for visible MRI lesions
 - D. Creates a 3D model of the surface of the brain
2. Multimodal imaging integration refers to:
 - A. Capturing fMRI at the time of a seizure
 - B. Co-registration of multiple imaging data in a common 3D space
 - C. Computational analysis of surface contours to detect subtle lesions
 - D. Computational analysis of gray-white matter boundary to detect subtle lesions
3. Which of these is the advantage of multimodal integration:
 - A. Automated process, less prone to human error
 - B. Combines multiple modalities to aid visualization in 2D and 3D
 - C. Aids the interpretation of epileptic networks based on the “anatomy-electro-clinical” concept
 - D. Post-operative scans can also be coregistered to visualize relationships between resection cavity and other imaging
 - E. All of the above

Answers may be found in the [Supporting information](#).